Three Dimensional Numerical Study on Droplet Formation and Cell Encapsulation Process in a T-Junction

Qiang Zhou, Hui Yang, L.-S. Fan

Department of Chemical and Biomolecular Engineering

The Ohio State University

Outline

Part 1: droplet formation

- Background: micro-droplet technologies
- Numerical Technique: LBM-IM
- Study of 3D droplet formation in T-junction
- Study of cell encapsulation in T-junction

Part 2: accurate simulation of gas-solid flow

- Background: Immersed boundary method
- IB-LBM: from first order to second order
- Numerical tests

Background: Micro-droplet technologies

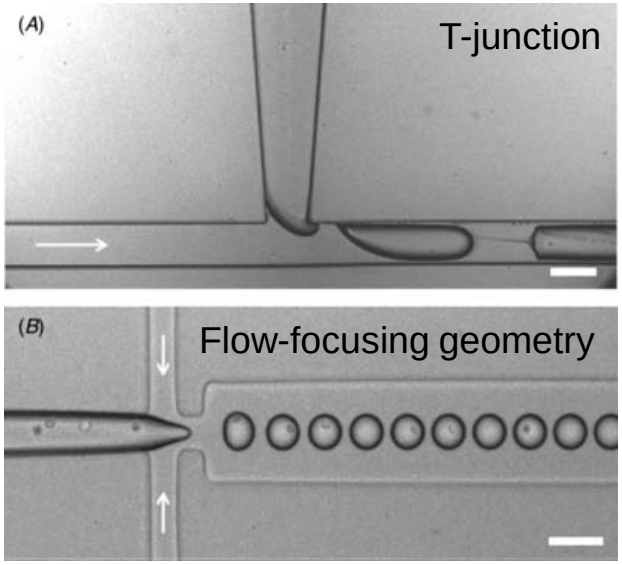

Hong et al. Biomed. Mater. **5** No 2 (April 2010) 021001 (6pp)

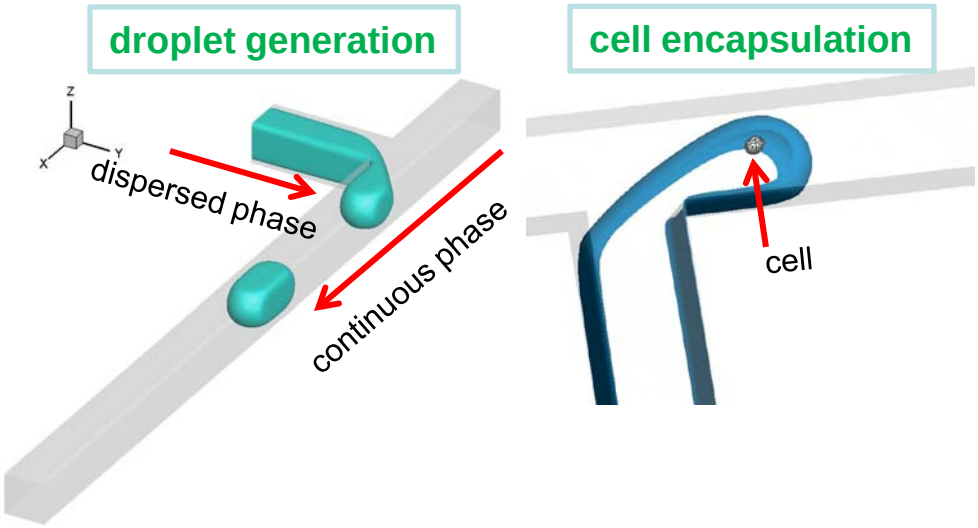

Droplets generated by microfluidic devices as micro reactors for cells

Applications: tissue engineering, food processing, drug delivery, tumor destruction, chemical reactions at the micron level (Christopher et al. 2007)

Two-processes:
droplet generation
cell encapsulation

Typical device: T-junction

Simulation Objectives:
Predict droplet size and address the droplet formation mechanism

Analyze the deformation of the cell in the process of encapsulation

Numerical Technique

Droplet formation simulation using Lattice Boltzmann Method (LBM)

(Shan-Doolen model,1995)

$$f_{ki}(\boldsymbol{x}+\boldsymbol{c}_i\delta_t,t+\delta_t)-f_{ki}(\boldsymbol{x},t)=-\frac{1}{\tau_k}\left[f_{ki}-f_{ki}^{(eq)}\right],\quad k=1,2$$

where, f_{ki} is the distribution function, from which we can compute the densities and the velocity fields.

Total intraparticle force acting on the kth component through interaction potential:

$$\boldsymbol{F}_k(\boldsymbol{x})=-\psi_k(\boldsymbol{x})\sum_{\bar{k}}G_{k\bar{k}}\sum_i\psi_{\bar{k}}(\boldsymbol{x}+\boldsymbol{c}_i\delta_t)\boldsymbol{c}_i$$

The influence of the interaction force is incorporated into the equilibrium velocity:

$$\boldsymbol{u}_k^{(eq)}=\boldsymbol{u}'+\tau_k\delta_t\frac{\boldsymbol{F}_k}{\rho_k}$$

Where the common velocity $\boldsymbol{u}'$ is defined obey the law of total momentum conservation,

$$\boldsymbol{u}'=\sum_k\frac{\rho_k\boldsymbol{u}_k}{\tau_k}\Big/\sum_k\frac{\rho_k}{\tau_k}$$

The mixed velocity of all components is also influenced by the interaction force:

$$\rho\boldsymbol{u}=\sum_k\rho_k\boldsymbol{u}_k+\frac{\delta_t}{2}\sum_k\boldsymbol{F}_k$$

Which makes the macroscopic governing equations closer to Navier-Stokes equations.

Numerical Technique:

3D simulation of droplet formation and cell encapsulation

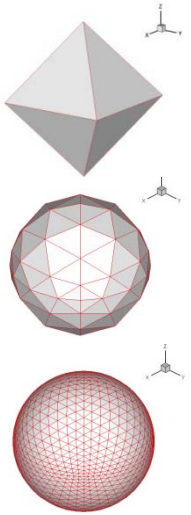

➢**Mesh generation for the cell**

unstructured mesh generation on sphere surface (Ramanujan and Pozrikidis 1998)

•Each triangular face of a regular octahedron is subdivided into 4n triangular elements.
•These elements are then projected radially outward onto its circumscribed sphere.
•Using this method, the mesh can be refined easily.

➢**Immerse Boundary (IB) Method (3D) is adopted**

➢**LBM equation with a force term**

$$f_{ki}(\boldsymbol{x}+\boldsymbol{c}_i\delta_t, t+\delta_t) - f_{ki}(\boldsymbol{x},t) = -\frac{1}{\tau_k}\left[f_{ki} - f_{ki}^{(eq)}\right] + \delta_t F_{ki}, \quad k = 1,2$$

An additional force density F_{ki} is applied to account for the interaction between the cell and the fluids around it.

Numerical Technique:

3D simulation of droplet formation and Cell capsulation

There are three contributions to the aforementioned force density:

- finite element solution of the in-plane tension (Sui et al 2008)

  Principle strains: λ_1 λ_2

  the first and second strain invariants $I_1 = \lambda_1^2 + \lambda_2^2 - 2,\ I_2 = (\lambda_1\lambda_2)^2 - 1$

  Strain energy function(neo-Hookean (NH) law)

$$W^{NH} = \frac{1}{6} E_s (I_1 - 1 + \frac{1}{I_2 + 1})$$

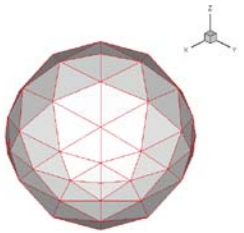

- Influence of bending stiffness (Tsubota, S. Wada 2010)

$$W_B = \frac{k_B}{2} \sum_{l=1}^{N} \tan^2(\frac{\theta_l - \theta_l^0}{2})$$

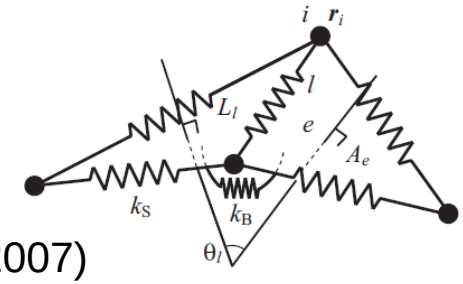

- Force due to the change of volume of the cell (Dupin et al 2007)

$$\boldsymbol{F}^V = -k_V \frac{V - V_0}{V_0} A\mathbf{n}$$

Study of 3D droplet formation in T-junction

Validation of the code for droplet formation

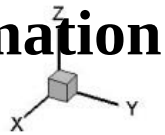

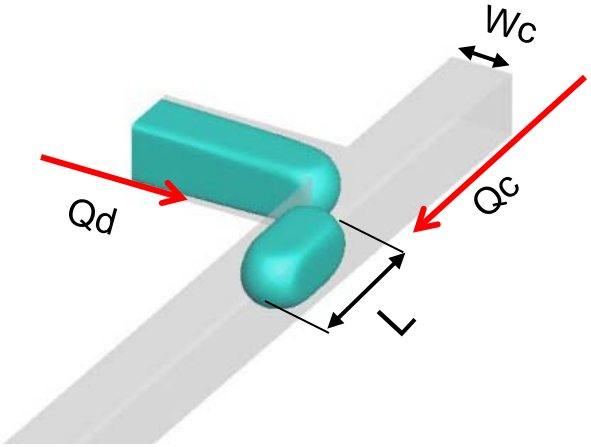

Important dimensionless parameters

$$Ca = \frac{\mu u}{\sigma} \qquad Q = \frac{Qd}{Qc}$$

The formula for the length of droplets for small Ca

L/Wc=a+bQ

was first proposed by Garstecki et al. (2006)

The variation of the length of the plug with Q for Ca =0.005 is shown; the data collapse onto the same straight line L/Wc=1+2Q. It's in good agreement with previous experimental and numerical work

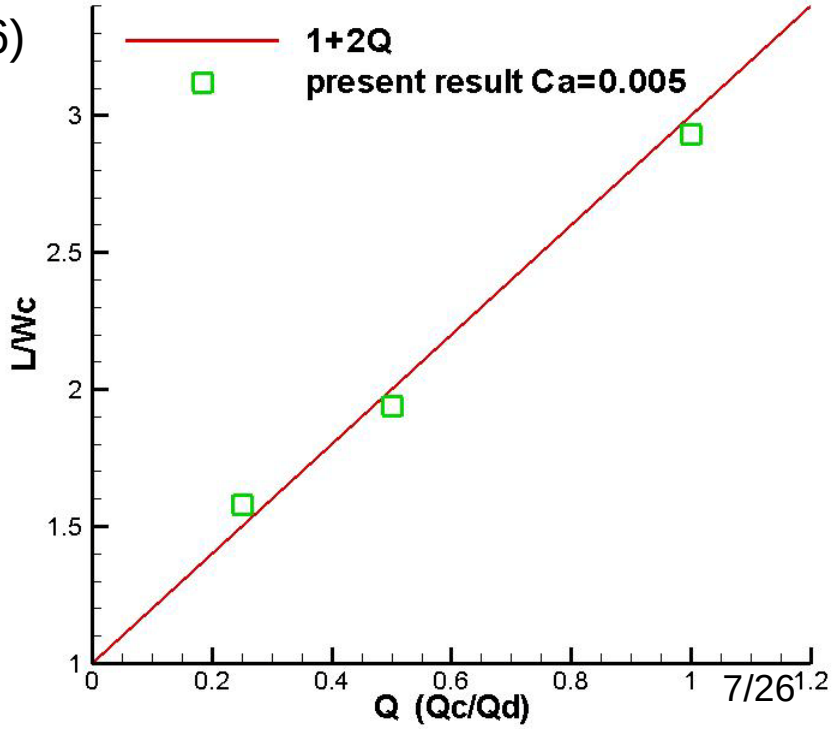

Study of 3D droplet formation in T-junction

Three regimes:

De Menech et al. (2008) identified, through a numerical investigation of the dynamics of break-up of immiscible fluids at a microfludic T-junction, three distinct regimes of formation of droplets(2D):

squeezing(Ca<0.005)

Dripping(0.005<Ca<0.03)

Jetting(Ca>0.03)

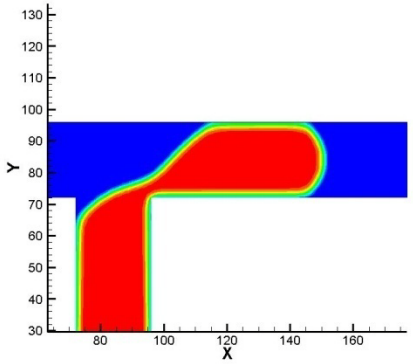

Squeezing

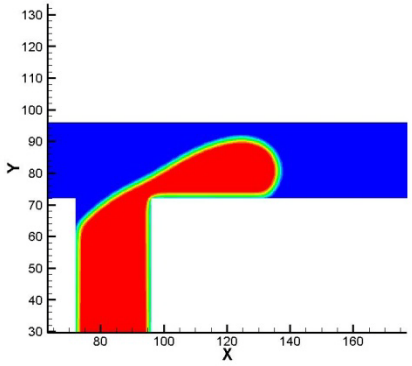

Dripping

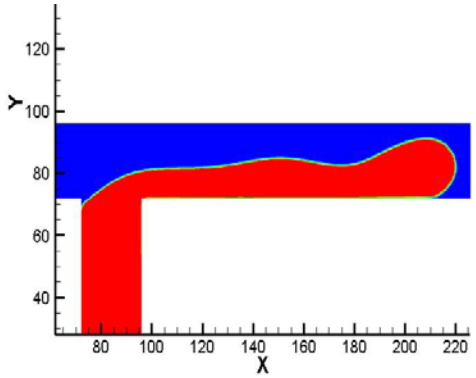

Jetting

Squeezing (Ca<0.01)

Ca=0.002 Q=0.25 λ=1

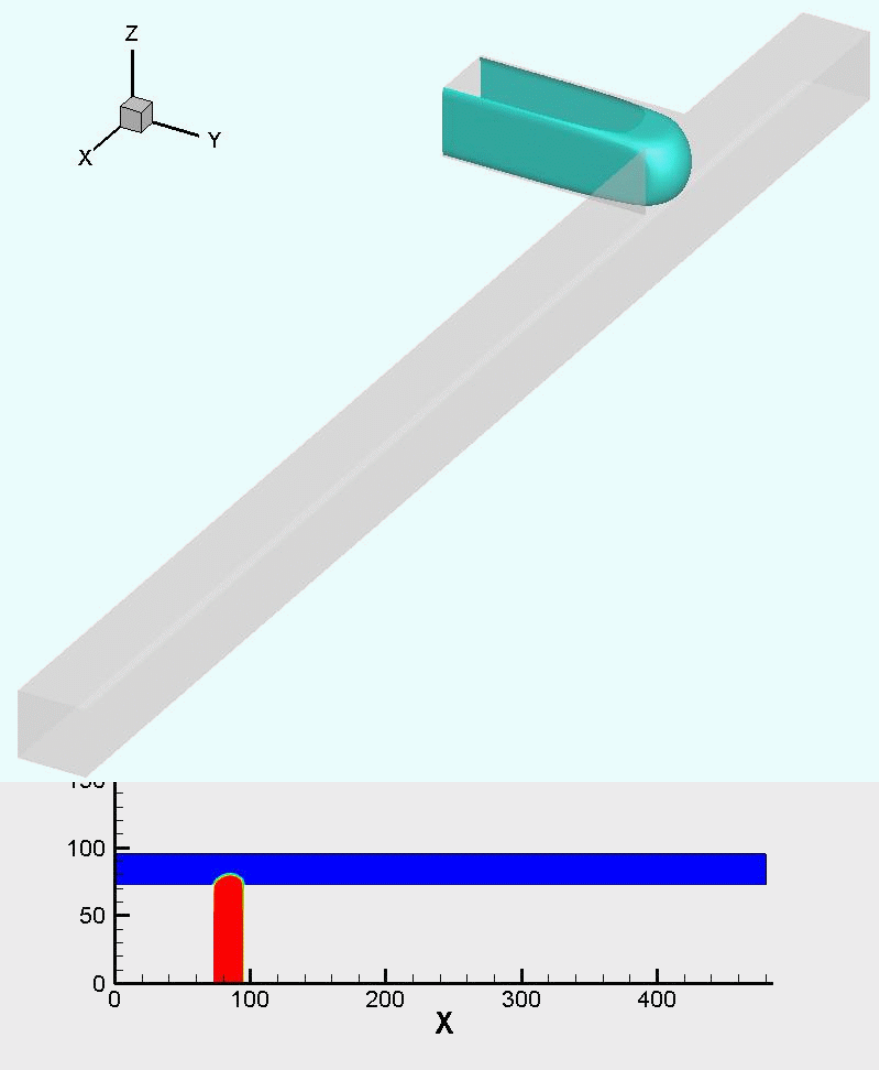

Block the whole channel before break-up to build enough pressure difference

The breakup point is always near the corner in this flow regime.

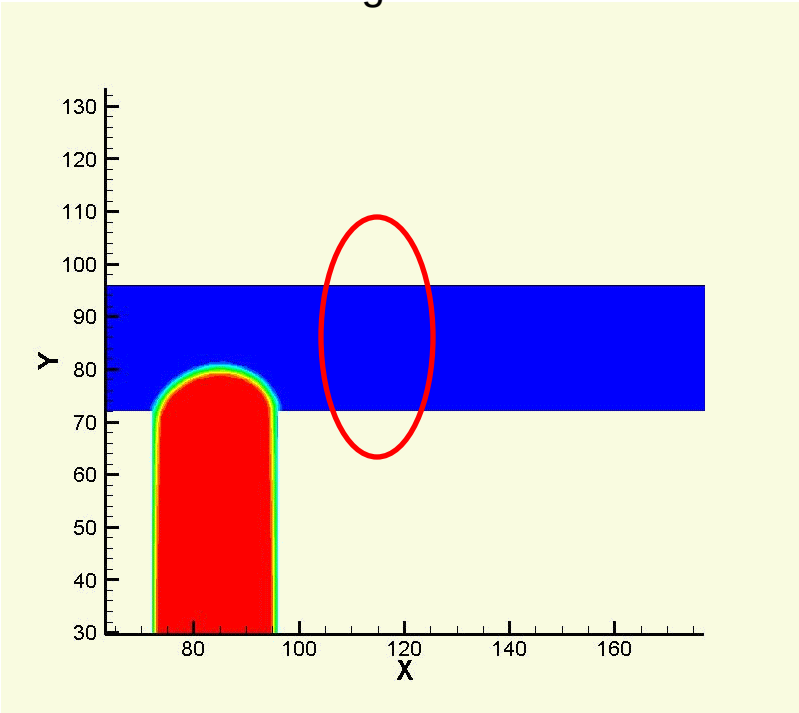

Squeezing (Ca<0.01)

Ca=0.002 Q=0.25 λ=1

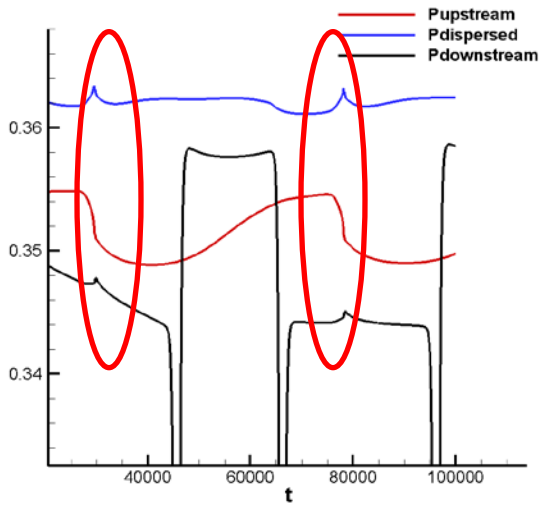

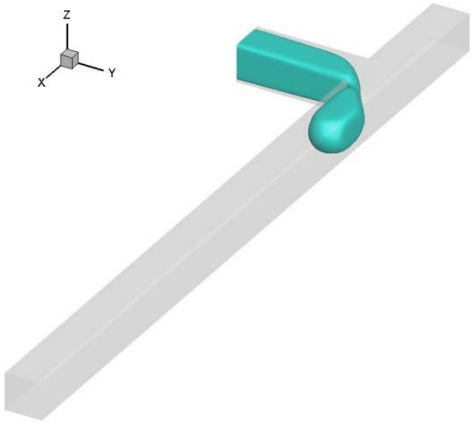

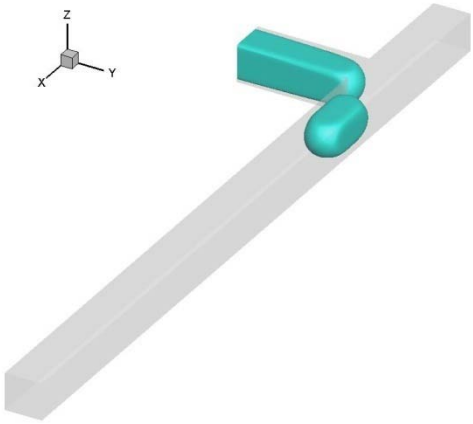

The pressure P upstream attains its peak before the breakup.
It decreases dramatically after breakup
Dp/p=1.5%

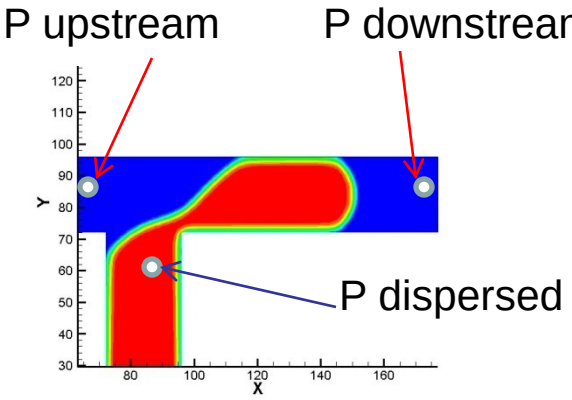

t=29000 (before breakup)

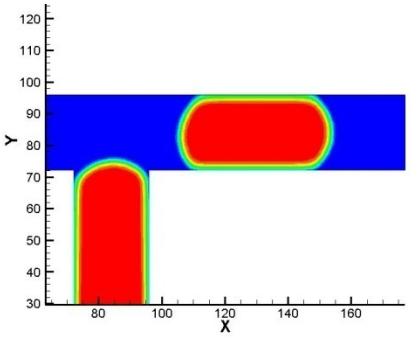

t=30000(after breakup)

Dripping (0.01<Ca<0.3)

Ca=0.01 Q=0.125 λ=1

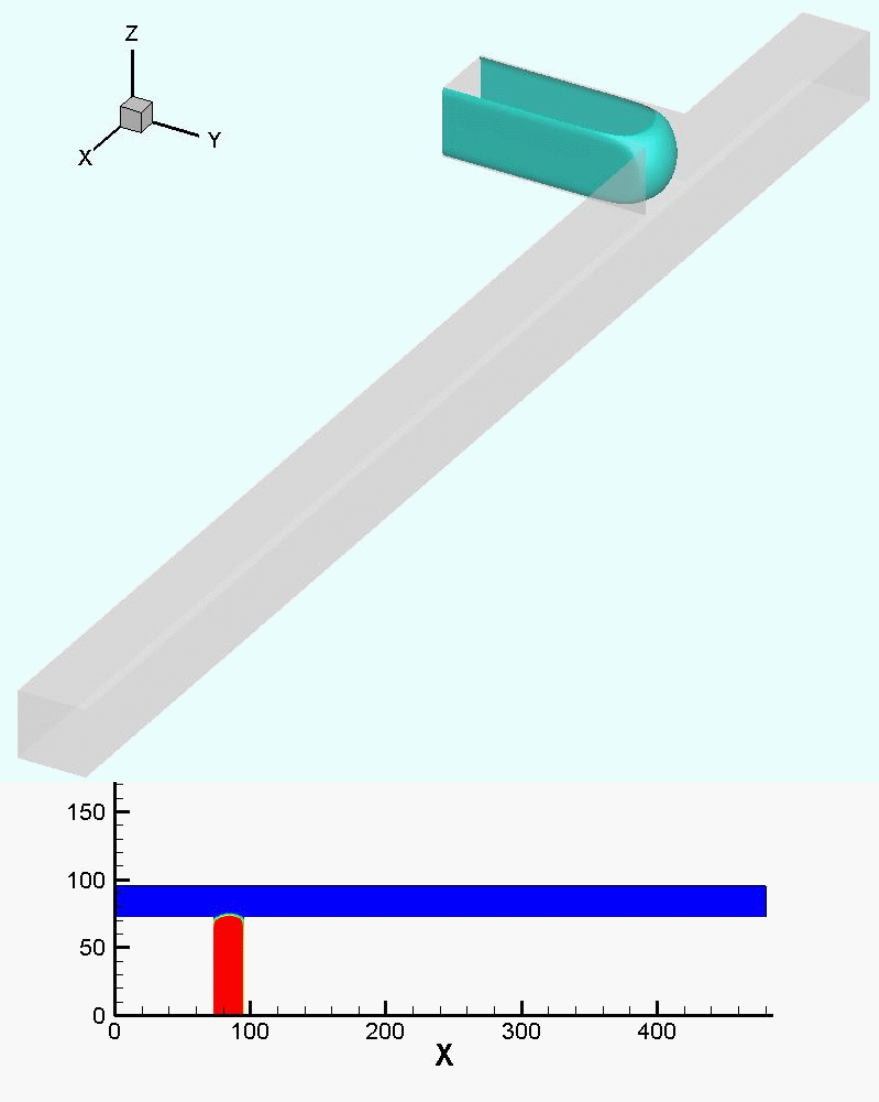

The droplet can not block the channel before its formation.
Shear stress become strong to cut off the droplet, pressure difference helps

The breakup point is also near the corner in this flow regime.

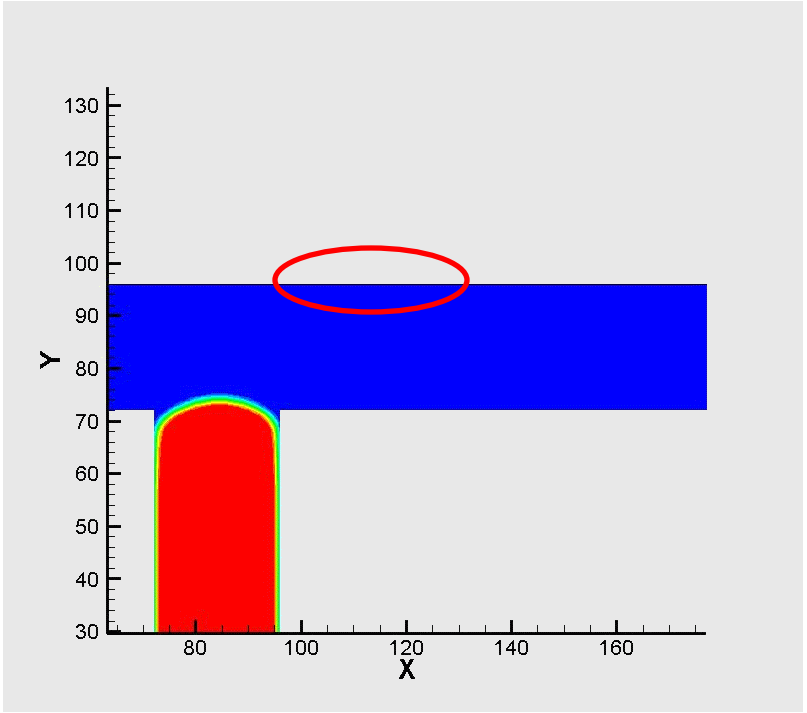

Dripping (0.01<Ca<0.3)

Ca=0.01 Q=0.125 λ=1

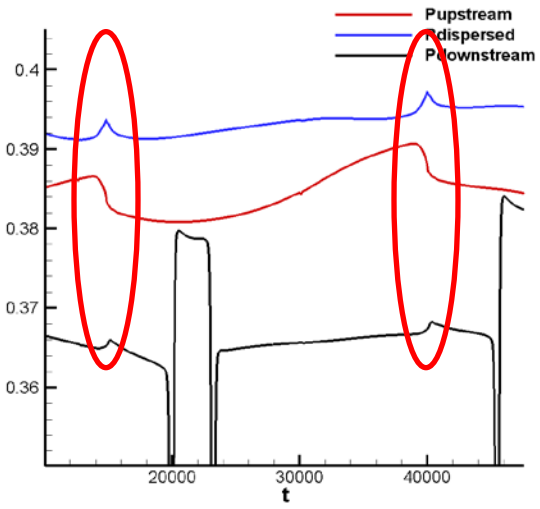

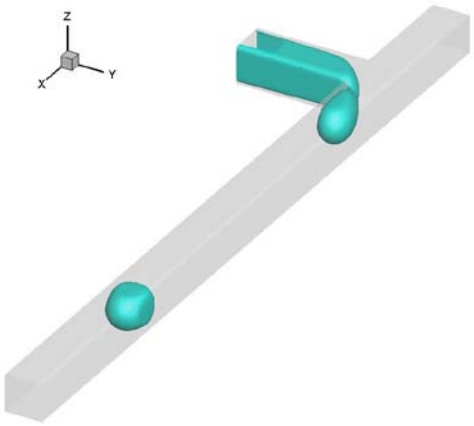

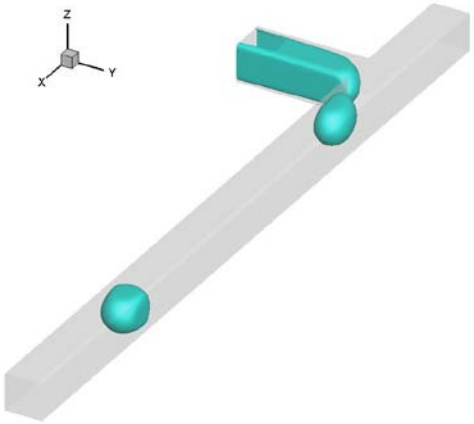

The pressure P upstream attains its peak before the breakup.
It decreases after breakup.
Dp/p=1.0%

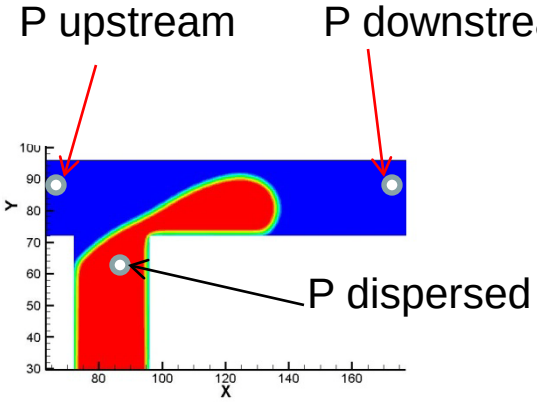

t=39500 (before breakup)

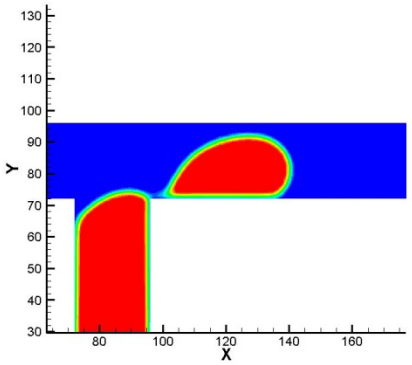

t=40000(after breakup)

Jetting (Ca>0.03)

Ca=0.056 Q=0.5 λ=1

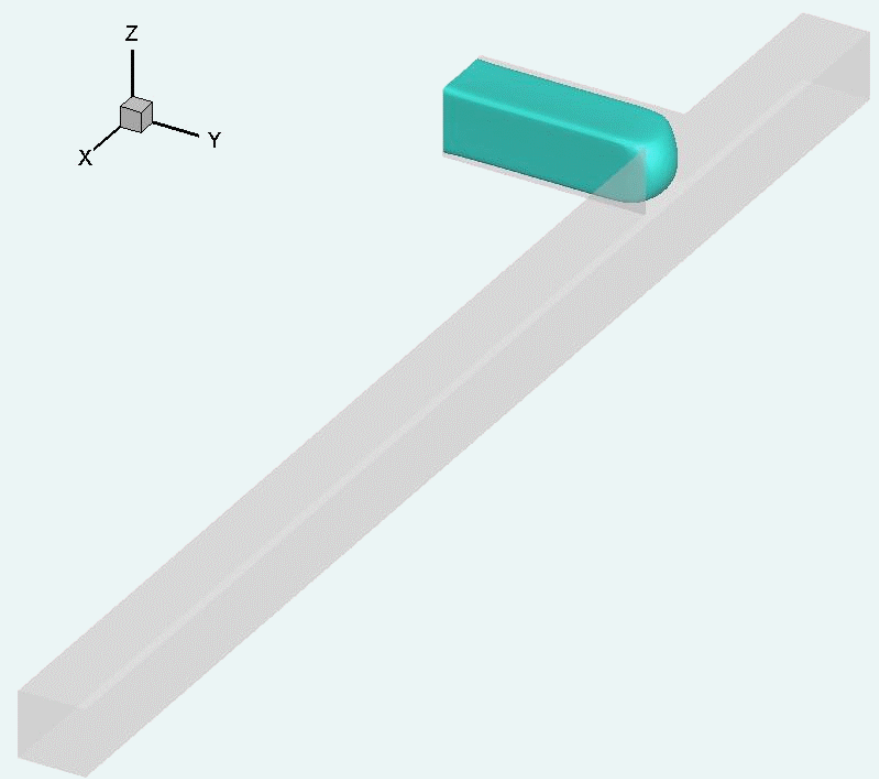

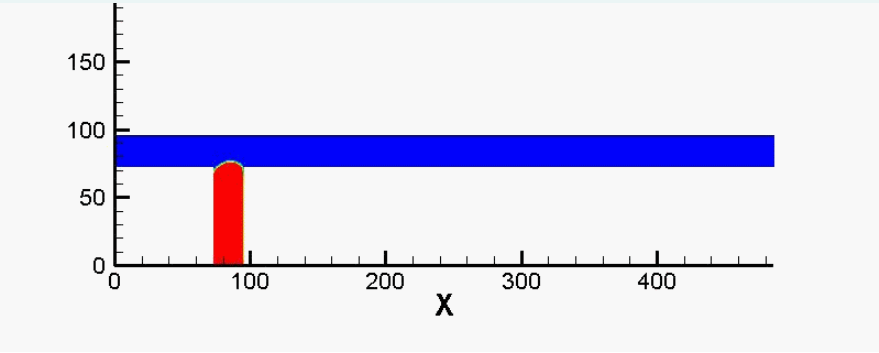

Shear stress become strong enough to cut off the droplet, the pressure difference is very small

The breakup point is in a location downstream of the junction.

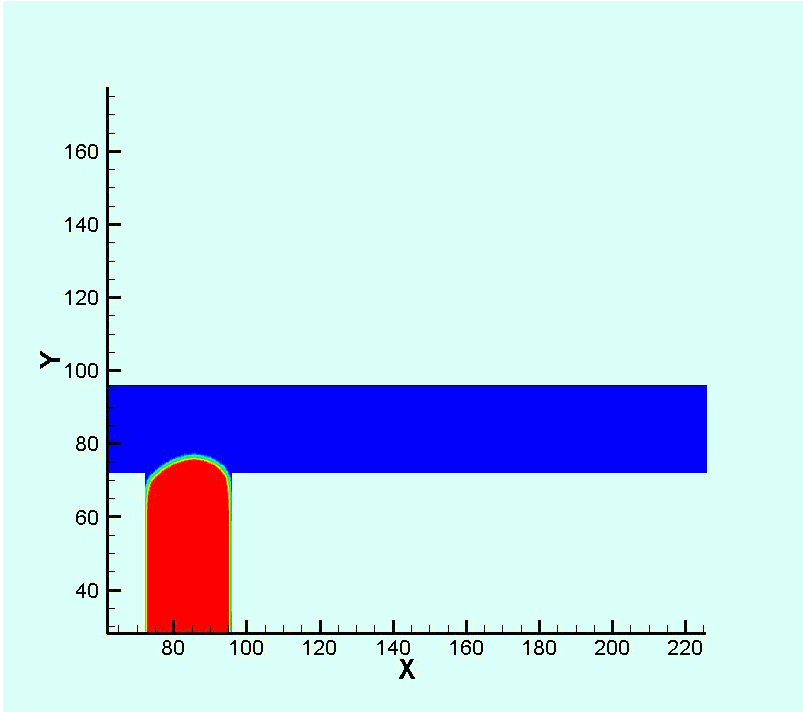

Jetting (Ca>0.03)

Ca=0.056 Q=0.5 λ=1

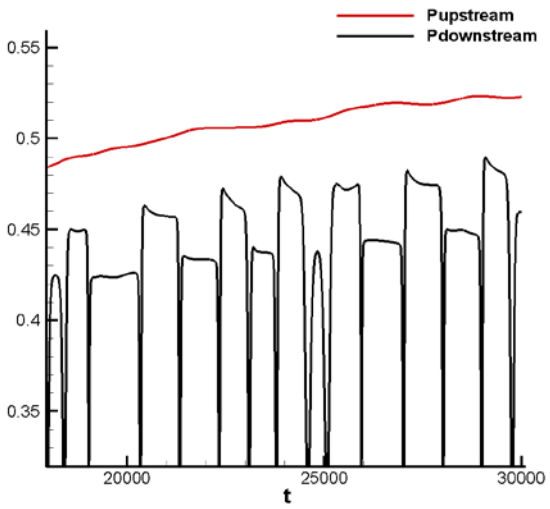

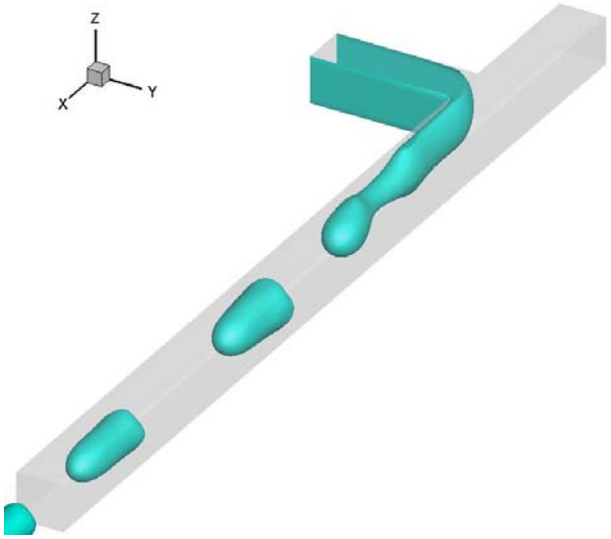

The pressure P upstream approaches to a constant value after the initial transient.

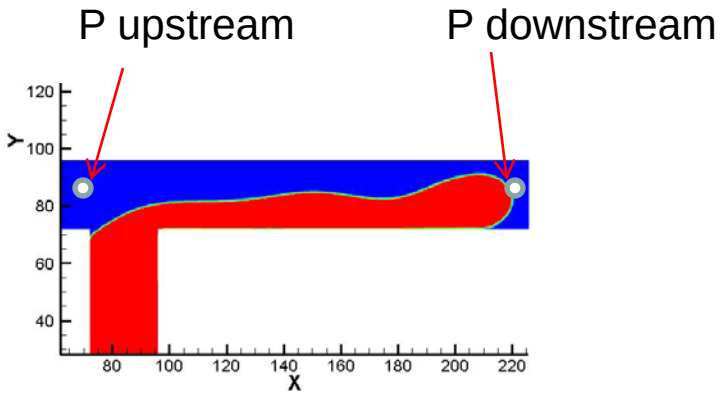

Study of cell encapsulation in T-junction

Validation of the code (only in-plane stress is considered, neo-Hookean (NH) law is adopted) $W^{NH} = \frac{1}{6} E_s (I_1 - 1 + \frac{1}{I_2 + 1})$ $G = \mu k a / E_s$

Taylor shape parameter $D_{xz} = (L - B)/(L + B)$

L **and** B **denote the semimajor and semiminor lengths of the cell in the plane of shear**

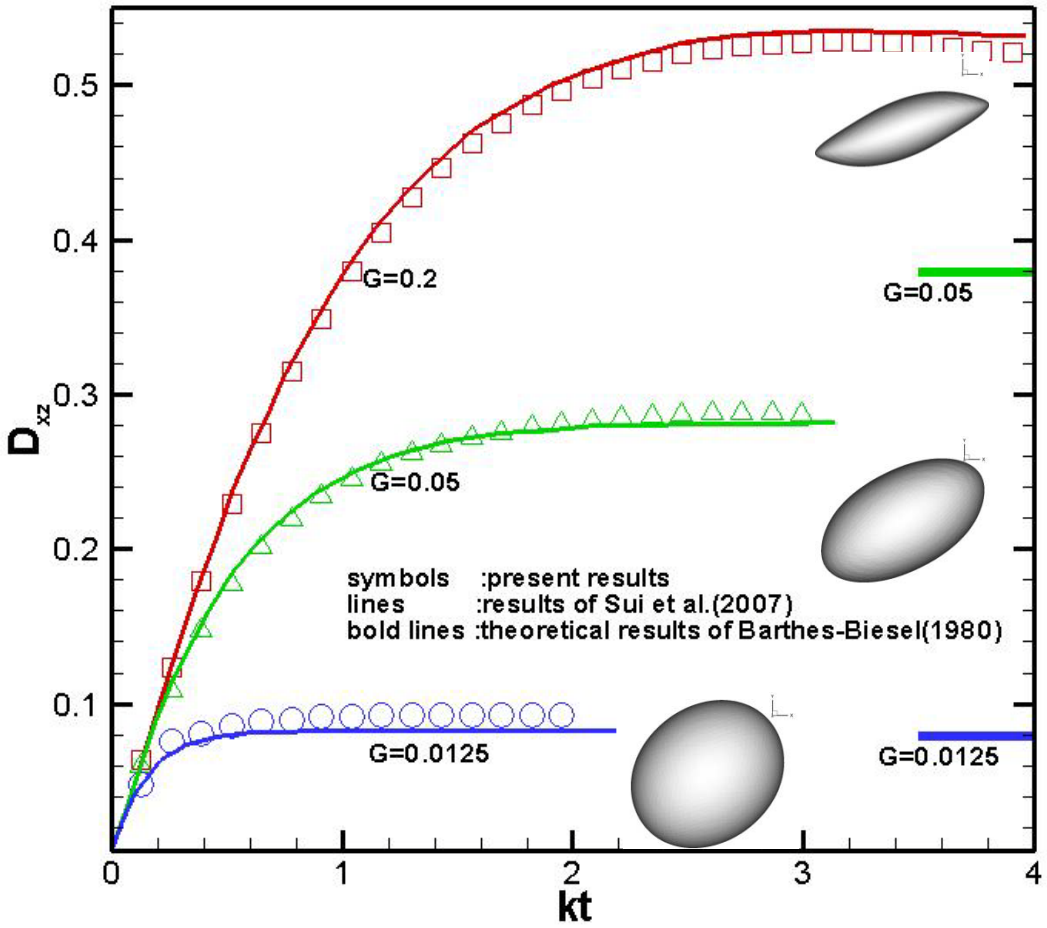

capsule deformation in simple shear flow

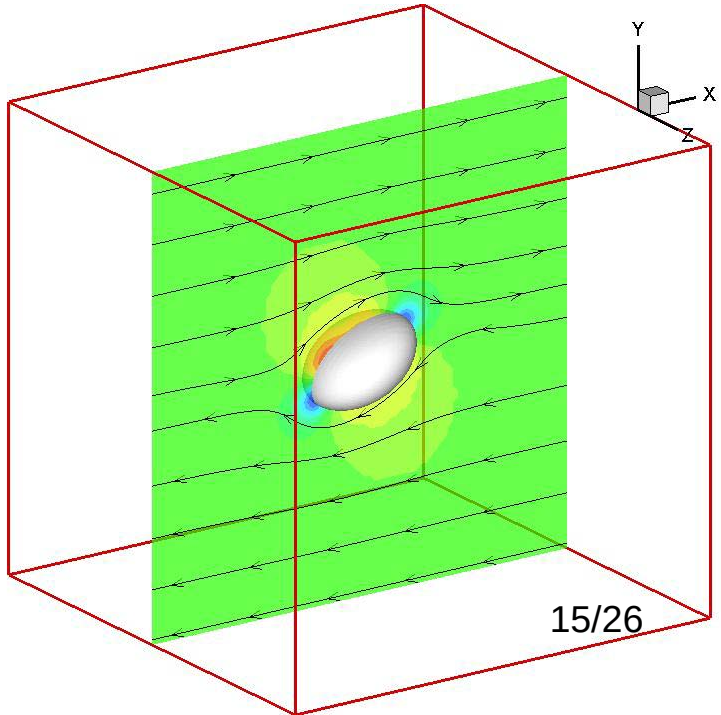

Study of cell encapsulation in T-junction

3D Ca=0.01 Q=0.25

G	Kb	Kv
0.25	1	1.2

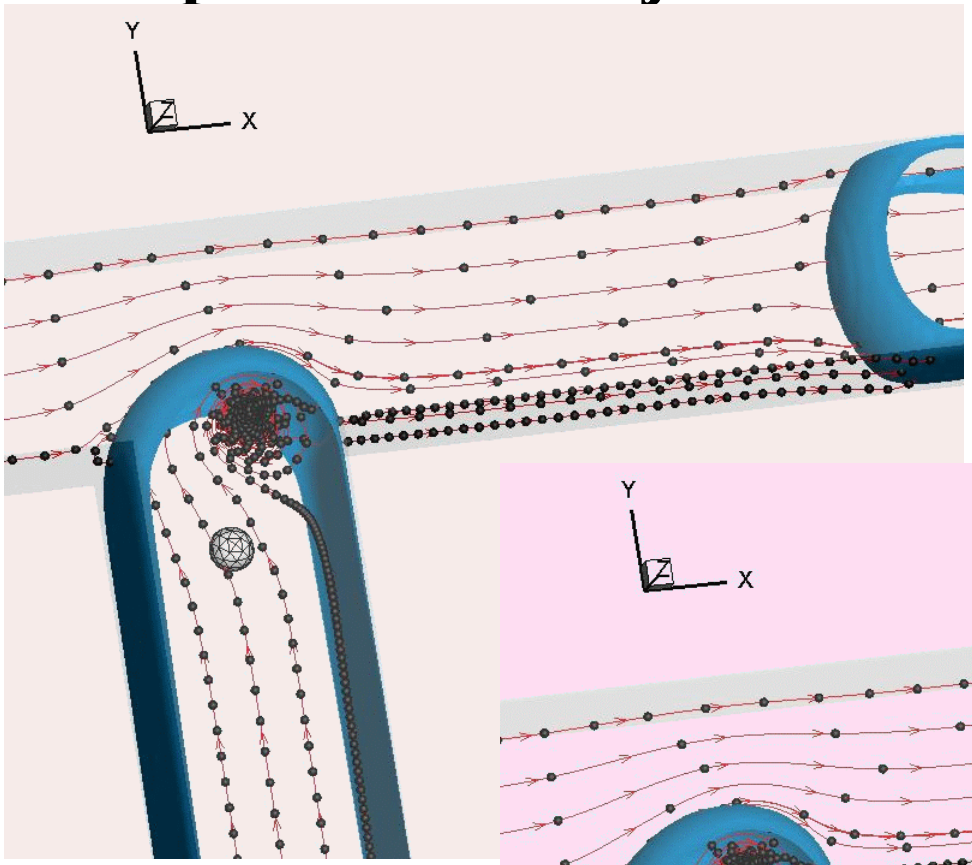

G	Kb	Kv
0.5	1	1.2

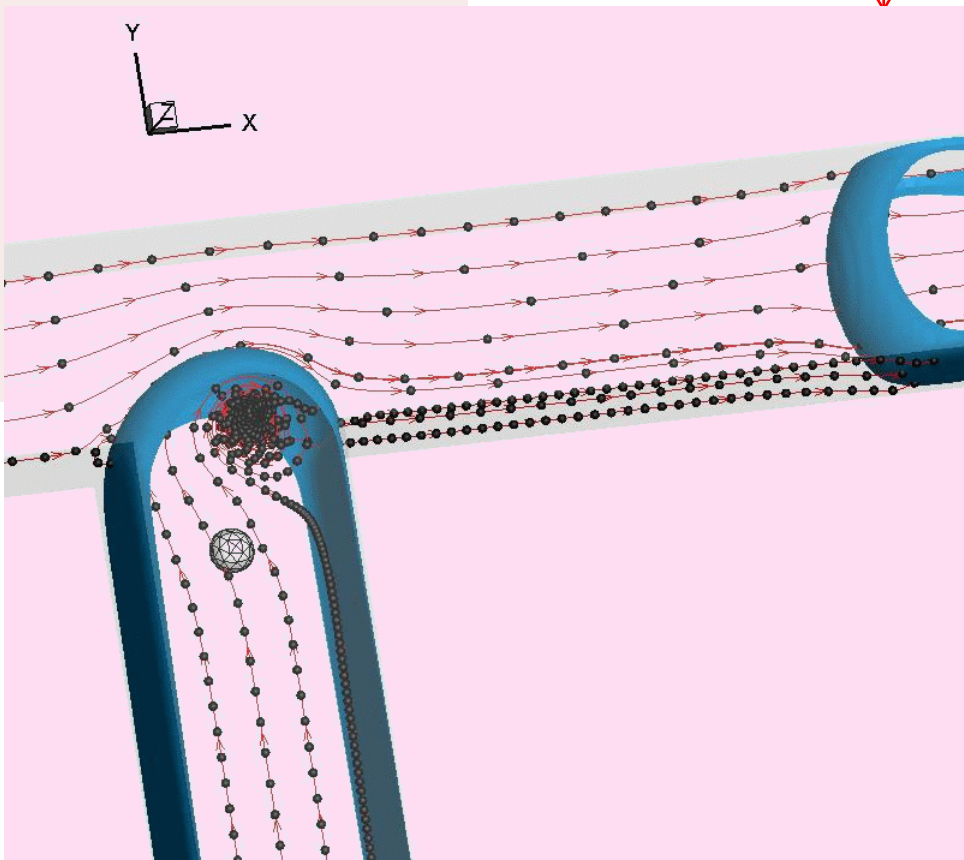

3D rotation is appreciable.

Study of cell encapsulation in T-junction

3D Ca=0.01 Q=0.25

Stretched by the flow

Larger G gives softer cell

Tank-treading mode of the cell during the encapsulation process can be observed clearly

The vortex near the corner makes the flow field complex

G Kb Kv
0.25 1 1.2

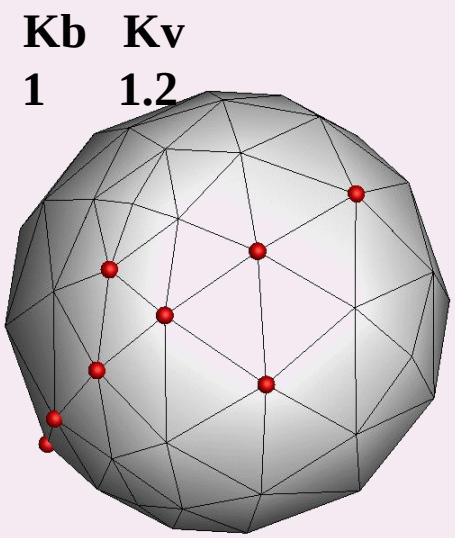

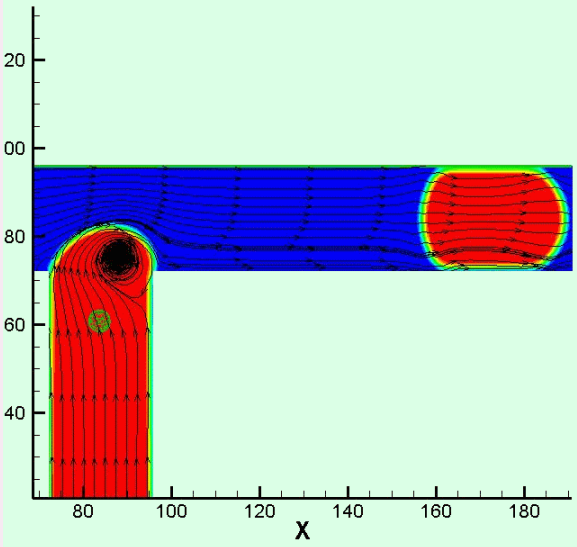

G Kb Kv
0.5 1 1.2

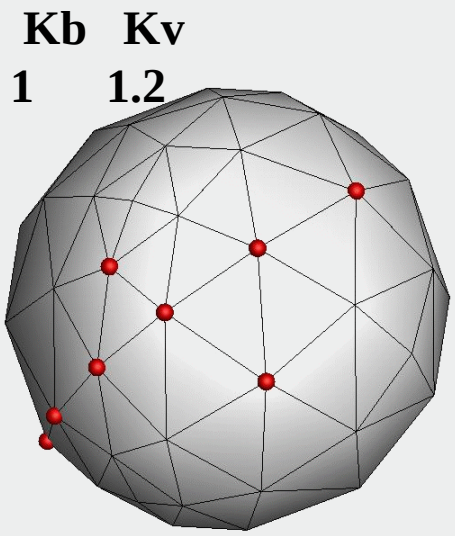

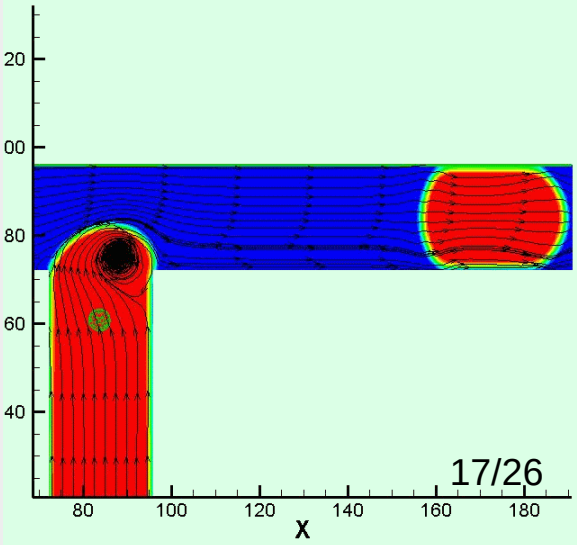

Part 2:
Background: the Immersed Boundary Method (IBM) for particulate flow

Advantage:

- The no-slip/no-penetration (ns/np) is easily imposed by adding additional force to the flow in the vicinity of the surface
- Does not need regridding when particles are moving

Disadvantage:

- The approximation of ns/np is hard to be exactly imposed.
- Traditional IBM only yields first-order accuracy.

Recent improvement by Breugem (2012)

- Multidirect forcing scheme to reduce the ns/np error (Luo et al. 2007)
- A slight retraction (Hofler and Schwarzer 2000) of the Lagrangian grid from the surface towards the interior of the particles is used to enhance the accuracy of IBM.

Breugem (2012) demonstrated that the improved IBM coupled with traditional incompressible NS-solver gives a second order of convergence

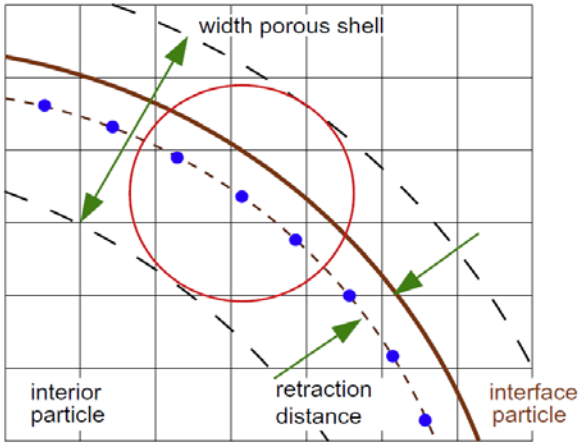

Fig. 3. Illustration of the porous shell covering a solid particle. The dots indicate the position of Lagrangian grid points, which are retracted from the actual interface (the solid line) with a fraction of the Eulerian grid spacing (about $0.3\Delta x$ in this case). The circle depicts the range of action of the regularized Dirac delta function.

Present work: embed the improved IBM into LBM

- Use relaxation technique to further reduce the ns/np error in the multi-direct forcing procedure

  change $\mathbf{u}^{**,s} = \mathbf{u}^{*} + \Delta t \mathbf{f}^{s}$ *to* $\mathbf{u}^{**,s} = \mathbf{u}^{*} + \Delta t(\mathbf{f}^{s-1} + \omega(\mathbf{f}^{s} - \mathbf{f}^{s-1}))$

- Using classic fourth order Runge-Kutta scheme to advance the position, the linear momentum and angular momentum of the particle. (Lower order Runge-kutta schems are under consideration since the fourth order scheme is sufficient to help the accuracy to reach second-order)

In the framework of LBM, we can not directly get the flow information in the fractional time step between $n\Delta t$ and $(n+1)\Delta t$. We get the flow information by simple extrapolation:

$$\mathbf{u}^{*} = \mathbf{u}^{n} + \alpha \Delta t(rsh^{n})$$

Numerical Test 1:Darcy problem (3D)
influence of retraction distance

- laminar flow through a simple cubic lattice of fixed spheres (Breugem (2012))
- The sphere is fixed in the center of the domain.

$$Da = \frac{\mu_f U_b}{(-dp_e/dx)D^2}.$$

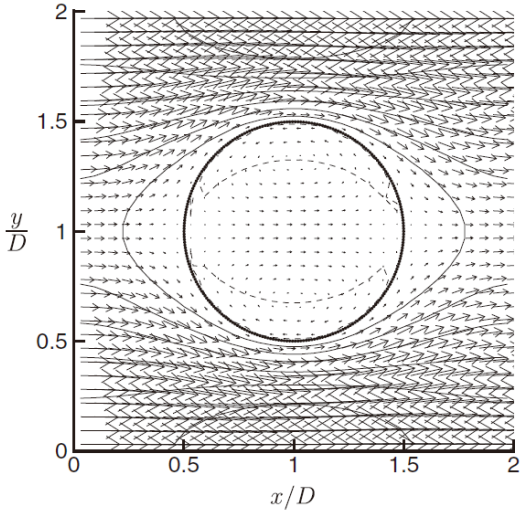

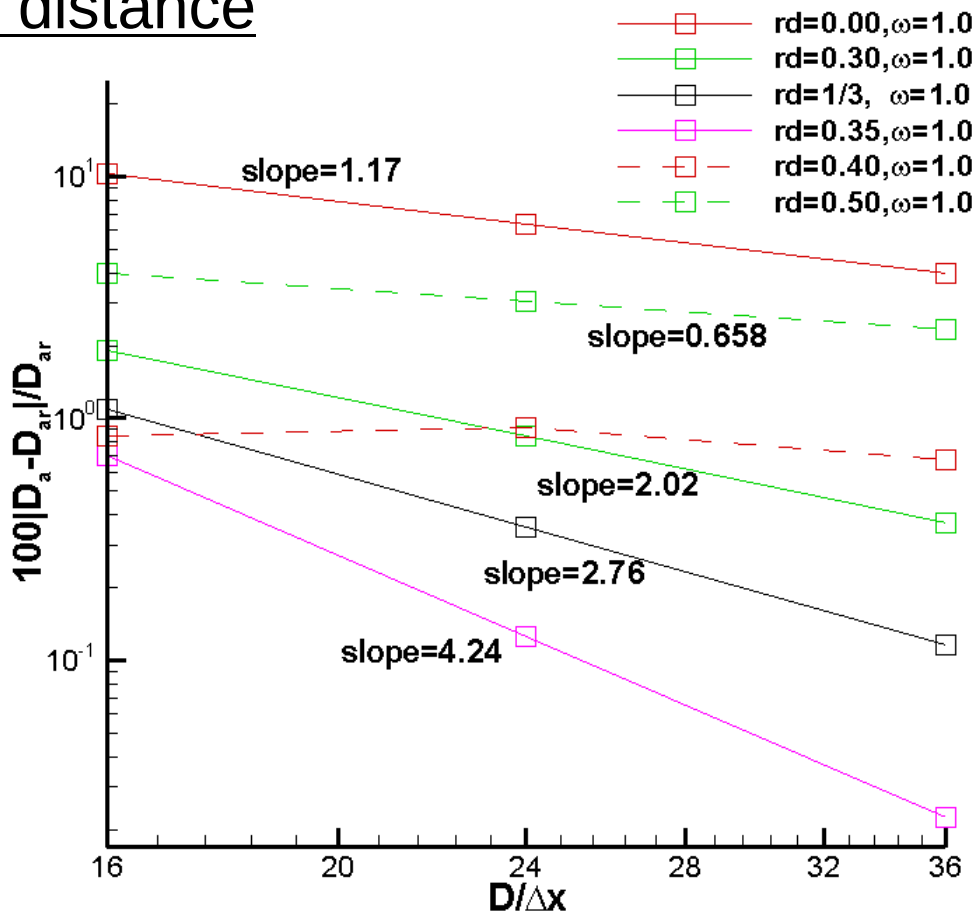

Convergence of the Darcy number

Numerical Test 1:Darcy problem (3D)
influence of relaxation coefficient

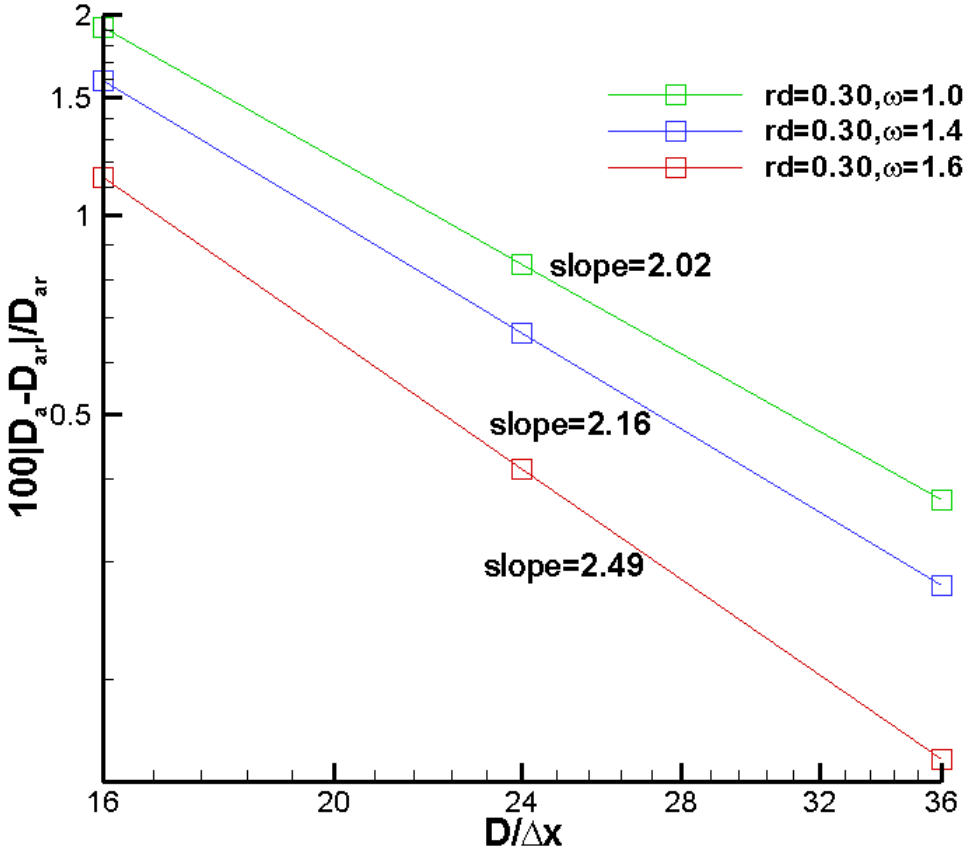

Convergence of the Darcy number

Numerical Test 2:Particle rotation in a simple shear flow

- Rotation-free but fixed in the position (Kempe and Frohlich (2012))

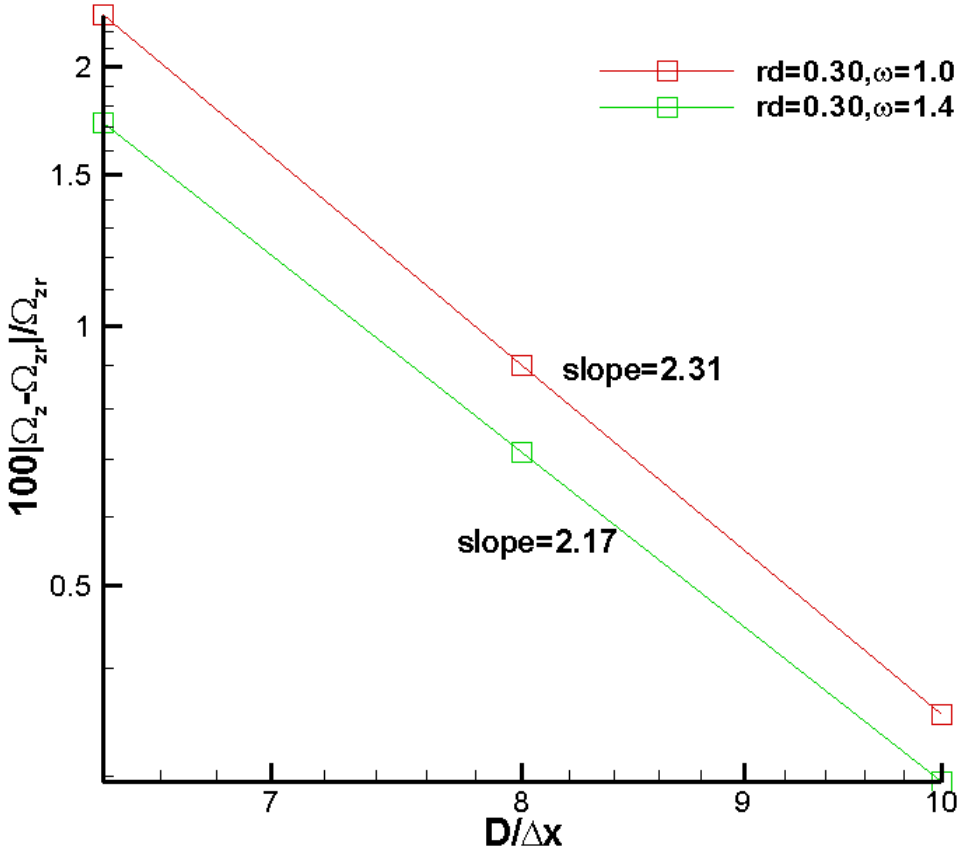

$$\mathbf{u}(y) = U_0 + Sy$$

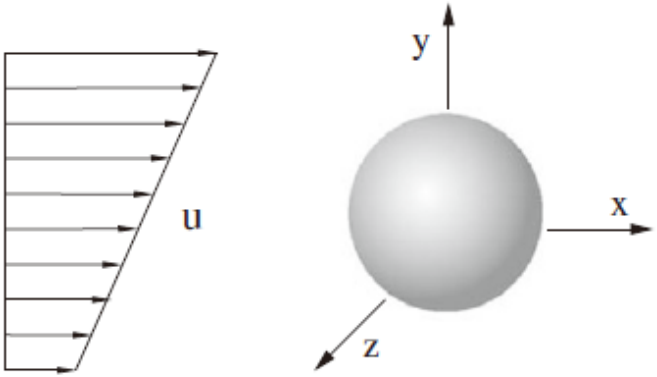

Convergence of the angular velocity

Numerical Test 3: Freely moving sphere in plane Poiseuille flow

- Free to translate and rotate (Uhlmann (2006))

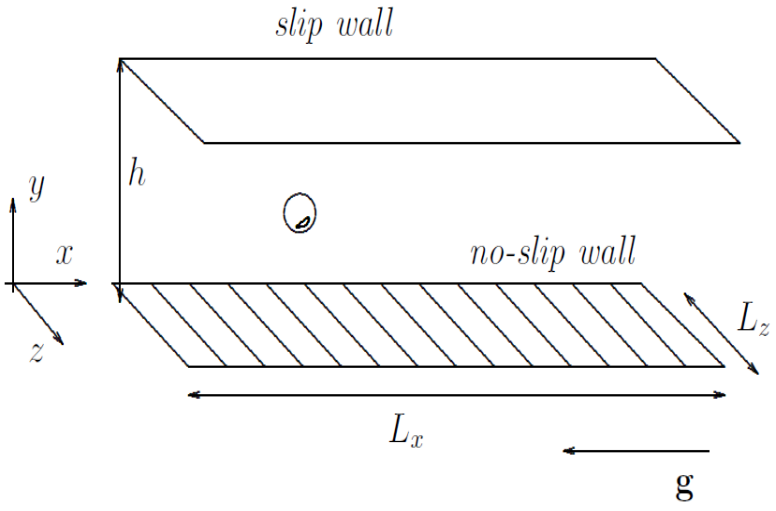

Schematic of the geometry for the case of particulate flow in a plane half-channel.

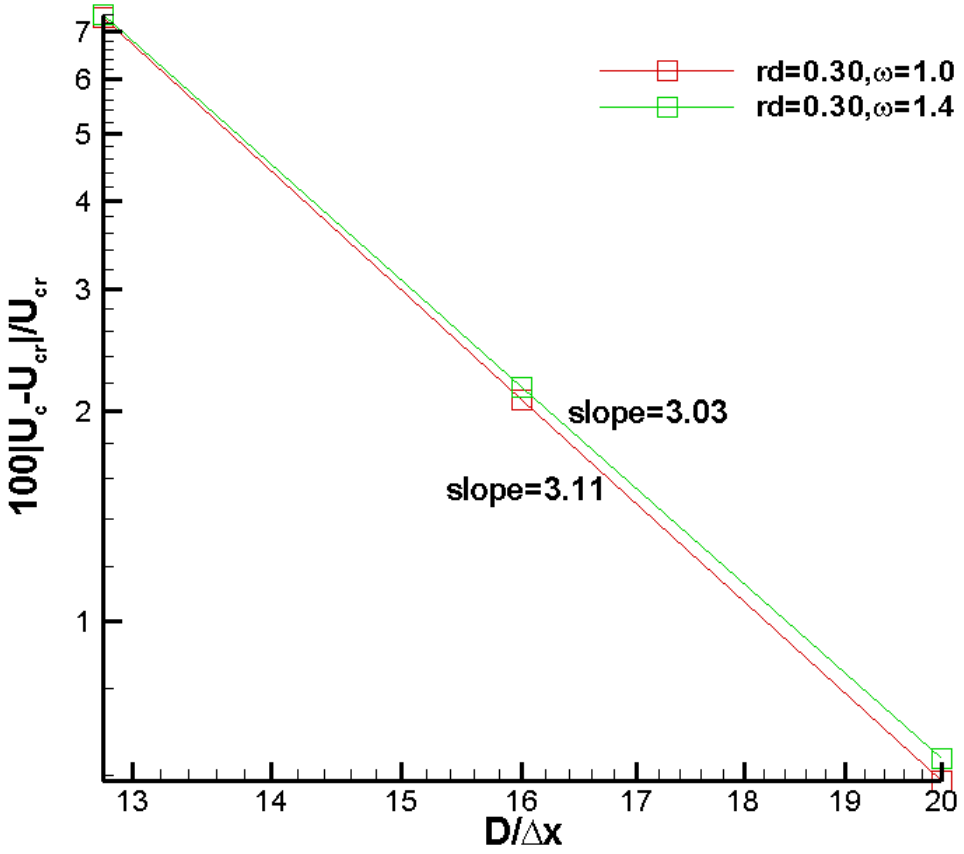

Convergence of the sphere velocity in x direction at the dimensionless time t=0.999

Concluding Remarks

- **Part 1**
- Three regimes of droplet formation (squeezing, dripping, jetting) are successfully simulated using 3D LBM method. The length of the droplet follows the scaling law developed by previous researchers.
- The constitutive properties of cell is developed by considering in-plane tension, bending moment and also the volume constraint. The cell capsulation process in 3D T-junction is simulated for the first time.
- **Part 2**
- Relaxation technique is applied to the multi-direct forcing scheme in IBM
- LBM and IBM is coupled through the classical fourth order Runge-kutta scheme. The overall accuracy reaches second-order. Super-convergence can be achieved (up to fourth-order) when retraction distance (0.30dx—0.35dx) and relaxation coefficient (1.4-1.6) are chosen properly.

Acknowledgement

- The first work is supported by the National Science Foundation Nano-scale Science and Engineering Center (NSF-NSEC).

- The second work is supported by HBCU award FE0007520 (Study of particle rotation effect in gas-solid flow using direct numerical simulation with a lattice Boltzmann method)